Molecular Cancer Therapeutics

Combined Cellular and Biochemical Profiling to Identify Predictive Drug Response Biomarkers for Kinase Inhibitors Approved for Clinical Use between 2013 and 2017

Joost C.M. Uitdehaag[1], Jeffrey J. Kooijman[1], Jeroen A.D.M. de Roos[1], Martine B.W. Prinsen[1], Jelle Dylus[1], Nicole Willemsen-Seegers[1], Yusuke Kawase[2], Masaaki Sawa[2], Jos de Man[1], Suzanne J.C. van Gerwen[1], Rogier C. Buijsman[1], and Guido J.R. Zaman[1]

Abstract

Kinase inhibitors form the largest class of precision medicine. From 2013 to 2017, 17 have been approved, with 8 different mechanisms. We present a comprehensive profiling study of all 17 inhibitors on a biochemical assay panel of 280 kinases and proliferation assays of 108 cancer cell lines. Drug responses of the cell lines were related to the presence of frequently recurring point mutations, insertions, deletions, and amplifications in 15 well-known oncogenes and tumor-suppressor genes. In addition, drug responses were correlated with basal gene expression levels with a focus on 383 clinically actionable genes. Cell lines harboring actionable mutations defined in the FDA labels, such as mutant BRAF(V600E) for cobimetinib, or *ALK* gene translocation for ALK inhibitors, are generally 10 times more sensitive compared with wild-type cell lines. This sensitivity window is more narrow for markers that failed to meet endpoints in clinical trials, for instance *CDKN2A* loss for CDK4/6 inhibitors (2.7-fold) and *KRAS* mutation for cobimetinib (2.3-fold). Our data underscore the rationale of a number of recently opened clinical trials, such as ibrutinib in *ERBB2*- or *ERBB4*-expressing cancers. We propose and validate new response biomarkers, such as mutation in *FBXW7* or *SMAD4* for EGFR and HER2 inhibitors, *ETV4* and *ETV5* expression for MEK inhibitors, and *JAK3* expression for ALK inhibitors. Potentially, these new markers could be combined to improve response rates. This comprehensive overview of biochemical and cellular selectivities of approved kinase inhibitor drugs provides a rich resource for drug repurposing, basket trial design, and basic cancer research.

Introduction

The theory of "oncogene addiction" postulates that, despite the diverse array of genetic lesions typical of cancer, some tumors rely on one single dominant oncogene for growth and survival (1). In the last two decades, the oncogene addiction model has been successfully translated into the design of personalized targeted therapies, particularly in the kinase field. Well-known examples include the EGFR kinase inhibitor gefitinib to treat lung cancers with activating mutations in *EGFR* (2), inhibitors of mutant BRAF (V600E) for metastatic melanoma (3), or ALK inhibitors to treat lung cancers characterized by transforming *ALK* translocations (4). Currently, 44 kinase inhibitors have been approved for clinical use by the FDA (status July 2018).

Despite these successes, the current markers of oncogene overactivity do not always correlate with clinical responses. For instance, one half of patients with melanoma positive for BRAF (V600E) responded to BRAF inhibitors and one half did not (5). Furthermore, mutations in the *PIK3CA* oncogene were not predictive of response to PI3K inhibitor therapy in breast cancer (6). This warrants a continued search for novel, more predictive drug response biomarkers. One of the best strategies to identify these is by profiling inhibitors in proliferation assays on cancer cell line panels (7, 8). Cancer cell lines faithfully resemble the mutations and gene expression features observed in primary biopsies (7), and all personalized therapies based on "oncogene addiction" can be reproduced in cell line models (7–9).

In order to understand clinical drug responses, and to rationalize their pharmacogenomic characteristics, it is important to understand the potency and selectivity of inhibitors. One of the earliest BRAF inhibitors, sorafenib, was insufficiently selective for BRAF to show clinical efficacy in BRAF(V600E)-mutant patients (10), which later was seen with the more selective inhibitors vemurafenib and dabrafenib (5). On the other hand, imatinib is approved for indications based on its polypharmacologic inhibition of ABL, KIT, and PDGFR kinases (11). Unfortunately, many kinase inhibitor potency values and selectivity profiles have been released only by the companies that market these inhibitors. Independent profilings on large kinase panels do not include all approved inhibitors (12). As a result, there is currently no independent head-to-head comparison of the kinase selectivity of all FDA-approved kinase inhibitors.

[1]Netherlands Translational Research Center B.V., Oss, the Netherlands. [2]Carna Biosciences, Inc., Kobe, Japan.

Note: Supplementary data for this article are available at Molecular Cancer Therapeutics Online (http://mct.aacrjournals.org/).

Corresponding Author: Guido J.R. Zaman, Netherlands Translational Research Center B.V., Kloosterstraat 9, 5349 AB Oss, the Netherlands. Phone: 31-412-700-500; Fax: 31-412-700-501; E-mail: guido.zaman@ntrc.nl

doi: 10.1158/1535-7163.MCT-18-0877

©2018 American Association for Cancer Research.

Downloaded from http://aacrjournals.org/mct/article-pdf/18/2/470/1860496/470.pdf by guest on 08 August 2023

Table 1. Biochemical characteristics of recently approved kinase inhibitor drugs

Generic name[a]	Trade name	Clinical use	Primary target	IC_{50} (nmol/L)	S_{sel}[b]	Secondary target	IC_{50} (nmol/L)	Tertiary target	IC_{50} (nmol/L)
Abemaciclib	Verzenio	$ER^+/HER2^-$ breast cancer	CDK4/CycD3	0.7	2.4	CDK6/CycD3	8.4	—	
Palbociclib	Ibrance	$ER^+/HER2^-$ breast cancer	CDK4/CycD3	1.1	1.0	CDK6/CycD3	3.9	—	
Ribociclib	Kisqali	$ER^+/HER2^-$ breast cancer	CDK4/CycD3	2.5	0.8	CDK6/CycD3	29		
Ceritinib	Zykadia	ALK-positive NSCLC	ALK	0.6	2.6	NPM1-ALK	0.7	IGF1R	9.77
Brigatinib	Alunbrig	ALK-positive NSCLC	ALK	0.6	3.3	NPM1-ALK	0.7	ROS	2.19
Alectinib	Alecensa	ALK-positive NSCLC	ALK	0.9	0.9	NPM1-ALK	1.0	—	
Acalabrutinib	Calquence	B-cell lymphoma	BTK	33	1.4	TEC	14	—	
Ibrutinib	Imbruvica	B-cell lymphoma	BTK	0.3	2.4	EGFR	17	HER2	16
Osimertinib	Tagrisso	EGFR(T790M)-mutant lung cancer	EGFR (T790M)	6.1	2.1	EGFR	25	—	
Neratinib	Nerlynx	HER2-positive breast cancer	HER2	43	1.6	EGFR	0.8	—	
Cobimetinib	Cotellic	B-RAF–mutant melanoma	MEK1	66	0.8	MEK2	352	—	
Copanlisib	Aliqopa	Lymphoma	$p110\alpha/p85\alpha$[a]	0.099	0.1	$p110\delta/p85\alpha$[c]	0.13	$p110\gamma/p85\alpha$[c]	0.097
Idelalisib	Zydelig	Lymphoma, CLL, SLL	$p110\delta/p85\alpha$[a]	0.60	0.04	$p110\alpha/p85\alpha$[c,d]	122	$p110\gamma/p85\alpha$[c]	14
Midostaurin	Rydapt	FLT3-mutant AML	FLT3	3.3	3.4	—		—	
Lenvatinib	Lenvima	Renal cell cancer	VEGFR2	1.3	2.0	VEGFR1	6.8	VEGFR3	1.83
Nintedanib	Ofev	Pulmonary fibrosis	VEGFR2	1.4	2.6	VEGFR1	12	VEGFR3	1.37
Tivozanib	Fotivda (EU only)	Renal cell cancer	VEGFR2	0.9	3.1	VEGFR1	3.3	VEGFR3	0.59

Abbreviations: AML, acute myeloid leukemia; CLL, chronic lymphocytic leukemia; NSCLC, non–small cell lung cancer; SLL, small lymphocytic leukemia.
[a]Order as discussed in this work.
[b]S_{sel} indicates selectivity entropy (14).
[c]Data from binding assay using SPR.
[d]Data from binding assay using SPR, taken from ref. 20.

In this study, we profiled 17 small-molecule kinase inhibitors (Table 1) that have been approved by the FDA in the past 4 years (from November 2013 to May 2018) on a panel of 280 biochemical kinase assays and a cell panel of 108 human cancer lines derived from various tumor tissues (Oncolines; ref. 13; Table 1). This follows up on an earlier study in which we profiled all kinase inhibitors approved prior to November 2013 (14). Fourteen of these 17 drugs were not included in previous comparative biochemical kinome profiling studies (12), although all except brigatinib and acalabrutinib were recently proteomically profiled (15).

Eight of the drugs are not included in any large-scale cell panel profiling studies such as the Genomics of Drug Sensitivity in Cancer (GDSC) and Cancer Therapeutics Response Portal (CTRP) databases (7–9). For the other nine, new, independently determined data are valuable, because cell line profiling data are known to be variable (8). The profiling data were used to analyze cellular responses using genomic (7, 8, 16) and transcriptomic (9, 17, 18) data. Novel markers of drug sensitivity were validated using the existing pharmacogenomic data from public sources. Our study provides unique insight into the relationship between biochemical and specific cellular responses of approved targeted therapy, and opens opportunities for wider application.

Materials and Methods

Kinase inhibitors

All kinase inhibitors were purchased from commercial vendors as summarized in Supplementary Table S1. Compounds were stored as solids at room temperature and dissolved in dimethyl sulfoxide before experiments.

Kinase profiling in enzyme activity assays

In total, 280 wild-type kinases were profiled in mobility shift, ELISA, and immobilized metal ion affinity particle (IMAP) assays as described earlier (Fig. 1A; Supplementary Table S2; refs. 14, 19). The compound concentration was 1 μmol/L, and the ATP concentration was within 2-fold of the $K_{M,ATP}$ for every individual kinase ($K_{M,bin}$). IC_{50}s were determined for primary and secondary kinase targets and for clinically relevant mutants. To quantify selectivity, selectivity entropies were calculated from percent inhibition values and measured IC_{50}s as described before (Table 1; ref. 14).

Kinase-binding assays

Binding of inhibitors on their primary targets was analyzed by surface plasmon resonance measurements on a Biacore T200 using biotin-tagged kinases as described (20).

Cancer cell lines

Cancer cell lines were obtained from the American Type Culture Collection (ATCC) from 2011 to 2017 and cultured in ATCC-recommended media. All experiments were carried out within ten passages of the original vials from the ATCC, who authenticated all cell lines by short tandem repeat analysis. Identity was verified by ascertaining the mutant status of 25 cancer genes from samples generated at Netherlands Translational Research Center B.V. (NTRC) (13).

Cell proliferation assays

Cell proliferation assays were performed as described (13, 14). In brief, cells were seeded in a 384-well plate and incubated for 24 hours. After addition of a dilution series of compound solution, the plates were incubated for an additional 72 hours followed by cell counting through use of ATPlite 1Step (Perkin Elmer). Percentage growth compared with uninhibited control was used for curve fitting to determine IC_{50}s and 50% lethal doses relative to the seeding cell density (LD_{50}s) as outlined before (Supplementary Table S3; ref. 13). IC_{50}s were used for all analyses because they better reproduced clinically validated biomarkers.

Cell line genetics

The mutation status of the cell lines was downloaded from the COSMIC cell lines project version 80 (https://cancer.sanger.ac.uk/cosmic; ref. 8). Only mutations, insertions, and deletions in recurrently mutated positions in tumor samples were considered (16). RL95-2 was annotated as mutant EGFR based on data from the Cancer Cell Line Encyclopedia (CCLE; ref. 21). Copy-number variations in the analyzed genes were also considered a

Downloaded from http://aacrjournals.org/mct/article-pdf/18/2/470/1860496/470.pdf by guest on 08 August 2023

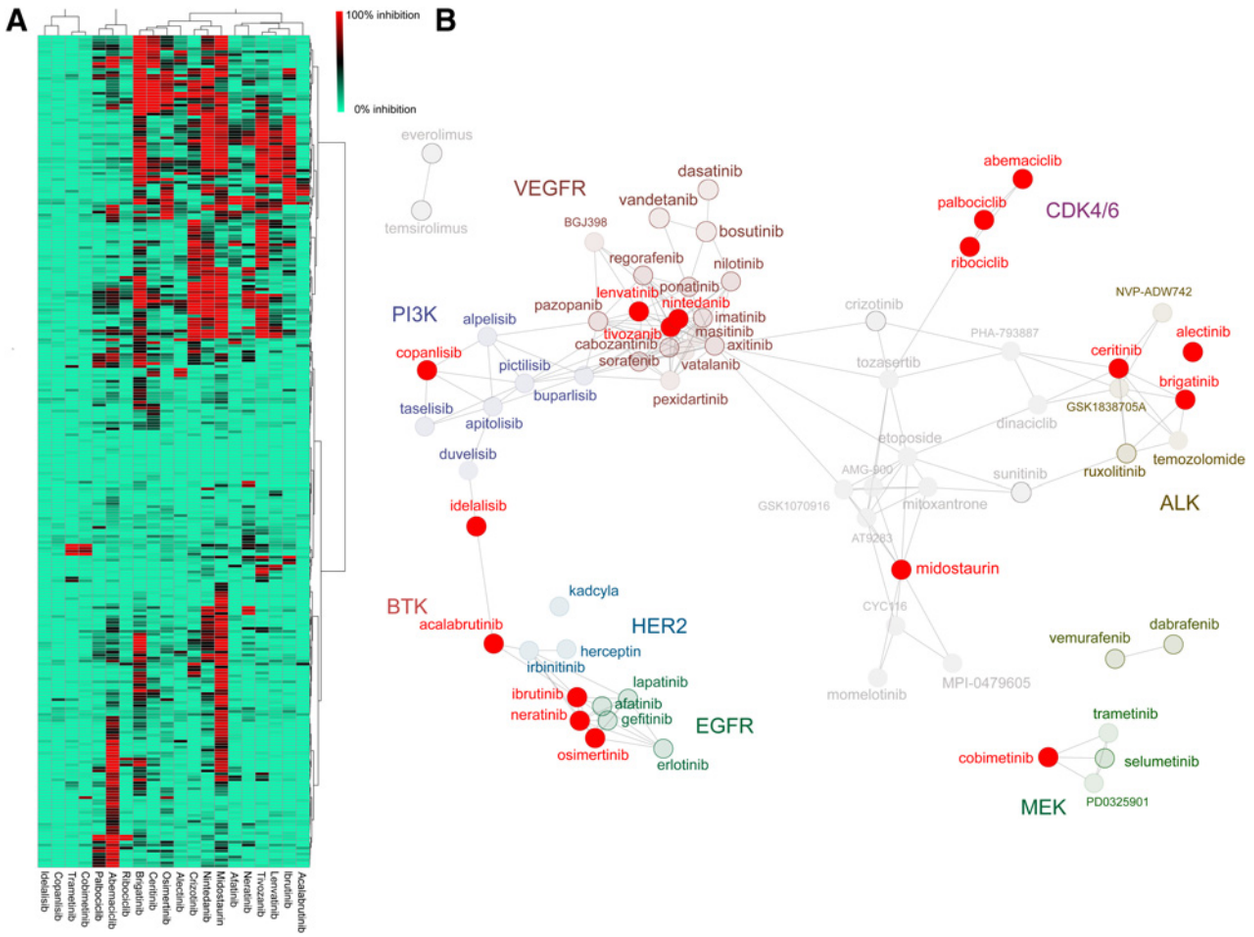

Figure 1.
Panel profiling of kinase inhibitors approved for clinical use. **A**, Ward-based clustering of biochemical inhibition profiles of 17 new inhibitors on 280 wild-type protein kinases. Previously published data of afatinib, crizotinib, and trametinib were included for completeness (14). **B,** Network tree based on cellular inhibition profiles. Nodes are linked if the Pearson correlation (r) $\geq$ 0.5 between inhibition profiles. The 17 new inhibitors are red. Previously FDA-approved kinase inhibitors and nonkinase inhibitors with $r \geq 0.5$ are included. Pastel colors indicate cluster identities based on hierarchical clustering.

mutation. ANOVA and multiple test corrections (significance limit $P_{adjusted} < 0.2$) were carried out in R as described previously (13). For a detailed workflow, see Supplementary Fig. S1.

Gene expression analyses

Gene expression profiles were downloaded for 18,900 genes for 94 of the 108 Oncolines cell lines, from the CCLE (7, 9), and correlated to drug response. First, Pearson correlations were calculated between expression levels and $^{10}\log IC_{50}$s. Analyzed genes were limited to 383 clinically actionable genes (as defined by DGIdb, version 3; ref. 22). Correlation scores were compared with the average correlations of 142 compounds profiled in the same cell panel (13) by Fisher z-transformation (9) and ranked. From this set, genes were highlighted blue that also showed significant ($P < 0.05$) correlations in at least 2 of 3 other mRNA expression databases [COSMIC (8), CCLE RNAseq (9), Genentech (17), which contain data for 102, 94, and 75 cell lines, respectively] and, when available, another IC_{50} data source such as the CTRP (v2.0; ref. 9) or GDSC database (v7.0; ref. 8), as incorporated in the PharmacoDB (v1.1; ref. 18). If genes could also be validated from compounds with similar molecular targets, they were highlighted in red. All analyses were done in R. For the workflow, see Supplementary Fig. S2. For results, see Supplementary Fig. S3A–S3Q. For results of the validation, see Supplementary Table S4.

Results and Discussion

To identify new potential applications of kinase inhibitors, we determined the biochemical potencies and selectivities of all approved kinase inhibitors since 2013 in a panel of 280 biochemical kinase assays (Fig. 1A). In addition, we generated the cell proliferation inhibition profiles in a tumor-agnostic panel of 108 cell lines (Fig. 1B). For the nine compounds that were profiled earlier, the average Pearson correlation with $^{10}\log IC_{50}$s in the GDSC or CTRP databases is 0.52, consistent with earlier reproducibility studies (8). A network tree based on cellular inhibition signatures clusters the kinase inhibitors according to the clinical distinction of their mechanisms (Fig. 1B). New approvals since 2013 have occurred in the area of CDK4/6, ALK, BTK, EGFR, HER2, MEK, PI3K, and spectrum-selective VEGFR inhibitors (red in Fig. 1).

Downloaded from http://aacrjournals.org/mct/article-pdf/18/2/470/1860496/470.pdf by guest on 08 August 2023

The CDK4 and CDK6 inhibitors ribociclib, palbociclib, and abemaciclib

Among the new approvals are three cyclin-dependent kinase 4/6 (CDK4/6) inhibitors: ribociclib, palbociclib, and abemaciclib (Table 1), which are used for treatment of hormone receptor–positive, HER2-negative breast cancer (www.fda.gov).

Abemaciclib is the most potent inhibitor of CDK4 in a biochemical enzyme activity assay (IC_{50} = 0.6 nmol/L), whereas palbociclib is the most potent on CDK6 (IC_{50} = 3.9 nmol/L). Ribociclib is 4 to 8 times less potent than the other two inhibitors (Table 1). This potency order is in line with the geometrically averaged IC_{50}s of abemaciclib, palbociclib, and ribociclib in the 108 cell line panel (Fig. 2) and consistent with a recent proteomic selectivity profiling study (15).

In the kinase assay panel, abemaciclib is the broadest spectrum CDK4/6 inhibitor, targeting 20 kinases at 1 μmol/L with > 95% inhibition, predominantly CDK2, 4, 6, and 9, CaMK2 isoforms, HIPK1-4, GSK3α and -β, PIM1-3, and DYRK1-3 (Supplementary Table S2). Under the same conditions, palbociclib only inhibits three kinases: CDK4/CycD3, CDK6/CycD3, and CLK1, and

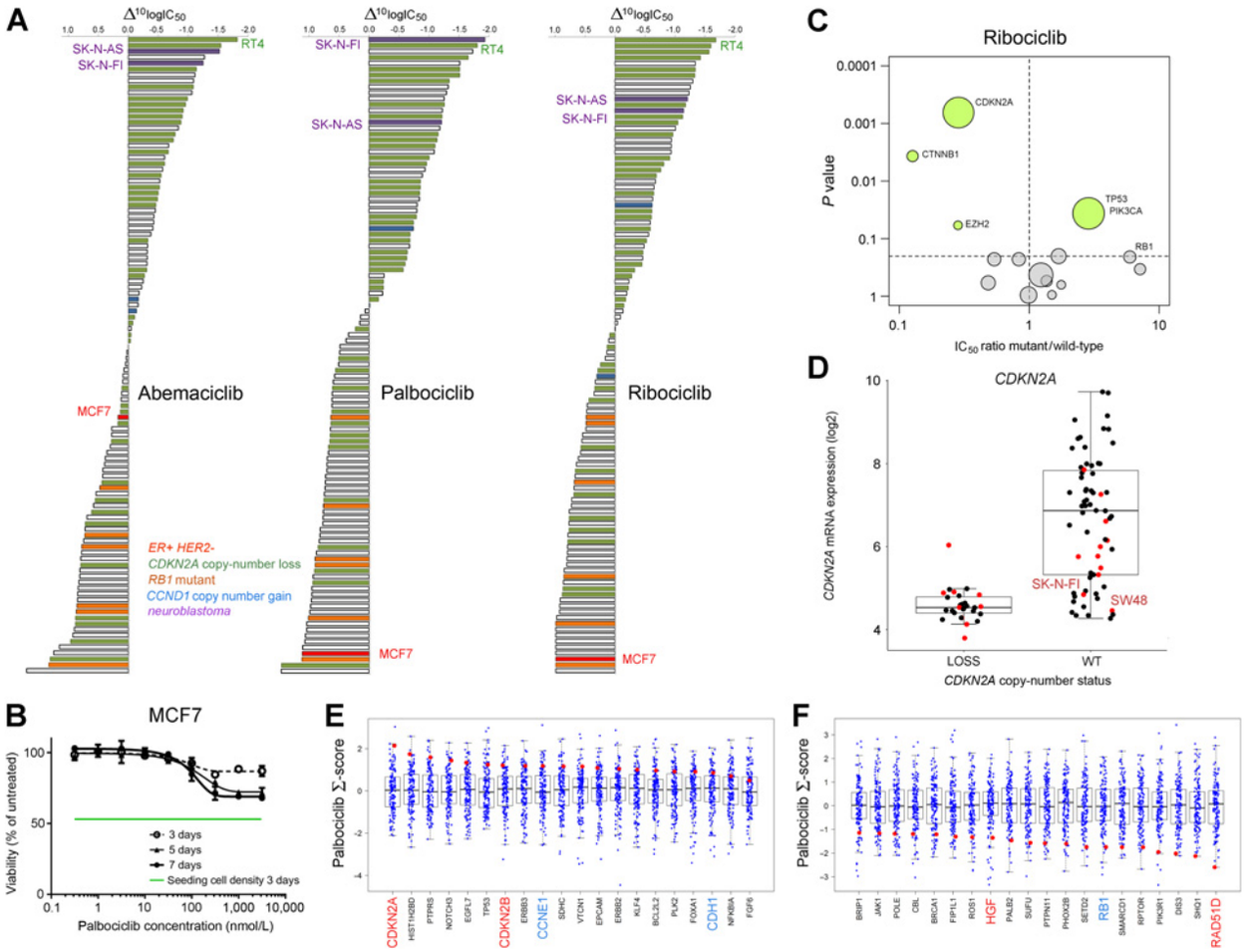

Figure 2.

Response biomarker analysis of CDK4/6 inhibitors. **A,** Waterfall plots of cellular ^{10}logIC_{50}s compared with the geometric panel average. The most sensitive lines are shown on top. Colors indicate the presence of previously observed response biomarkers. Geometrically averaged IC_{50}s are 640 nmol/L, 1,120 nmol/L, and 3,360 nmol/L for abemaciclib, palbociclib, and ribociclib, respectively. **B,** The response window in the MCF7 proliferation assay depends on incubation time, as illustrated for palbociclib. For clarity, only the cell seeding density for the 3-day assay is shown. Seeding densities for the 5- and 7-day assays were 40% and 33% of final viability. **C,** ANOVA analysis relating ribociclib response to hotspot cancer gene mutations and copy-number variations in cell lines. Genes with $p_{adjusted} < 0.2$ (dotted line) are colored green. Circle areas are proportional to number of cell lines with variations in the gene. *x* axis IC_{50} ratio < 1 indicates sensitivity. *x* axis IC_{50} ratio > 1 indicates resistance. **D,** Cell lines with normal *CDKN2A* copy numbers can show low mRNA expression levels. The top 20 CDK4/6 inhibitor–sensitive cell lines (on average) are colored red. The sensitive lines SW48 and SK-N-FI have low *CDKN2A* mRNA levels but no genomic *CDKN2A* loss. **E,** Correlation analysis of drug sensitivity with basal gene expression levels in the cell lines. Only clinically actionable genes with significant Pearson correlations are shown ($P < 0.05$). In this example, palbociclib (red circles) is compared with the score of 142 other inhibitors (blue circles). Correlations were Fisher-z transformed and normalized to a Σ-score. A positive score indicates that low mRNA expression correlates with low (potent) ^{10}logIC_{50}. The 20 highest scoring genes are shown. Gene names highlighted blue indicate correlations that remain significant ($P < 0.05$) after cross-validation with at least 2 of 3 alternative gene expression sources and that are significant in an earlier palbociclib profile (PharmacoDB; ref. 18). Genes highlighted red meet the same validation requirements also in the abemaciclib or ribociclib profiles. **F,** As in **E**, but the top 20 most negative scores, indicating correlations between high mRNA expression and low (potent) ^{10}logIC_{50}.

Downloaded from http://aacrjournals.org/mct/article-pdf/18/2/470/1860496/470.pdf by guest on 08 August 2023

ribociclib only two: CDK4/CycD3 and CDK6/CycD3. To quantify selectivity based on the overall 280-kinase profile, we calculated the selectivity entropies, which summarize a panel profile in a single value (14). These label abemaciclib as moderately selective ($S_{sel} = 2.4$) followed by the highly selective palbociclib and ribociclib ($S_{sel} = 1.0$ and $S_{sel} = 0.8$, respectively). This order is identical to earlier profiling experiments (15, 23, 24).

During clinical trials, it appeared that the dose-limiting toxicity (DLT) of abemaciclib is fatigue, whereas the DLT for the other two compounds is neutropenia (25). This different clinical profile has been attributed to abemaciclib's higher activity on CDK4 compared with CDK6 (25). However, in the biochemical assays, all three CDK4/6 inhibitors are 3- to 10-fold more potent on CDK4 than on CDK6 (Table 1). Potentially, the neutropenia observed for palbociclib and ribociclib could be related to CDK4/6 inhibition and be counteracted by inhibition of some additional kinase by abemaciclib. A good candidate would be GSK3β inhibition, which leads to Wnt activation, resulting in enhanced proliferation of bone marrow progenitor cells and ultimately neutrophils (26). Abemaciclib is a potent inhibitor of GSK3β (Fig. 1A; 95% at 1 μmol/L) and was shown to be able to activate Wnt signaling, in contrast to the other CDK4/6 inhibitors (27).

New response biomarkers for CDK4/6 inhibitors

Various biomarkers have been tested in clinical trials, such as loss of *CDKN2A*, amplification of *CCND1*, and presence of wild-type *RB1* (28), although none were included in the final label. Indeed, in the Oncolines panel, *CDKN2A* loss is strongly predictive of CDK4/6 inhibitor sensitivity, and cell lines with mutations in *RB1* are consistently more resistant (Fig. 2A). For ribociclib, *CDKN2A*-mutant and *RB1*-mutant lines are 2.7 and 5.9 times more sensitive and insensitive, respectively. Also the finding that CDK4/6 inhibitors are particularly effective in neuroblastoma is confirmed (ref. 29; Fig. 2A).

The $ER^+/HER2^-$ breast cancer cell line MCF7, which best represents the current patient population for these inhibitors, is only moderately sensitive to CDK4/6 inhibitors compared with the other cell lines (Fig. 2A). Because work by others indicated that CDK4/6 inhibitors need extended incubation times, we also performed the proliferation assays for 5 and 7 days (30). This indeed improves IC_{50}s, but not in such a way that the MCF7 cell line becomes especially sensitive (Fig. 2B). It should be kept in mind, however, that clinically, CDK4/6 inhibitors are coadministrated with antiestrogens or aromatase inhibitors, which synergistically enhance their activity (30).

To find additional response biomarkers, we performed ANOVA based on mutations and copy-number variations in known cancer hotspots in the cell lines and the measured drug responses (Supplementary Fig. S1). The analysis confirms *CDKN2A* and shows *CTNNB1* and *EZH2* mutations as significant sensitivity markers (Fig. 2C; Supplementary Fig. S3A–S3C). *TP53* mutation is a resistance marker (Fig. 2C), consistent with the clinical observation that breast cancer patients with mutations in *TP53* are generally less responsive to abemaciclib (31). Other significant resistance markers are mutations in *PIK3CA* (for ribociclib) or *PTEN* (for abemaciclib and palbociclib) which both lead to activation of the PI3K pathway. PI3K pathway activation is also an adaptation in acquired CDK4/6 inhibitor resistance (32).

In addition, we searched for gene expression–based markers. To limit the number of false positives, we only considered clinically actionable genes and normalized correlations relative to the profiles of 142 other anticancer agents. This yielded a list of expression-based response markers (Fig. 2D–2F). Top scoring genes were validated by recalculating correlations using experimentally independent gene expression data and IC_{50} datasets (red and blue in Fig. 2E and 2F).

The most significant mRNA-based sensitivity marker is low *CDKN2A* expression (Fig. 2D and 2E). Interestingly, some sensitive cell lines, such as SK-N-FI and SW48, harbor wild-type *CDKN2A* at the DNA level, but have low *CDKN2A* mRNA levels, suggesting both are independent markers (Fig. 2D). High *RB1* expression is confirmed as sensitivity marker (Fig. 2F). Novel gene expression–based sensitivity markers, which reach significance for at least two of three inhibitors, are high expression of the DNA repair protein *RAD51D* and the hepatocyte growth factor *HGF*, and low expression of *CDKN2B* (Fig. 2E and F). Also interesting is high *CCNE1* expression as a resistance marker for palbociclib (Fig. 2E), which was also reported recently (30).

The ALK inhibitors ceritinib, brigatinib, and alectinib

The first anaplastic lymphoma kinase (ALK) inhibitor, crizotinib, was approved in 2011. Since then, three new ALK inhibitors were approved: ceritinib, brigatinib, and alectinib. The indication for all inhibitors is ALK-positive non–small cell lung cancer, which originates from an ALK-activating gene rearrangement such as EML4-ALK or NPM-ALK. In addition, crizotinib has shown activity in ALK-positive lymphoma, but has not been registered for this indication yet (33).

Profiling in the 280 biochemical kinase assay panel shows that alectinib is the most selective ALK inhibitor, with a selectivity entropy (S_{sel}) of 0.9 and inhibiting only four kinases with >95% at 1 μmol/L: ALK, LTK, MSSK1, and CHK2. Ceritinib and brigatinib inhibit, respectively, 16 and 48 kinases in the panel and have S_{sel} values of 2.6 and 3.3, indicating medium to low selectivity. In our earlier profiling study (14), crizotinib inhibited 28 of 313 kinases ($S_{sel} = 2.7$).

Biochemically, ceritinib binds most strongly to ALK, closely followed by brigatinib, whereas alectinib and crizotinib are less potent. This is apparent from the biochemical assays (Table 1) but especially in ALK-binding assays using surface plasmon resonance (SPR; Fig. 3A). Also the inhibitory IC_{50}s in assays of common ALK activation and resistance mutants show this order (Fig. 3B). This shows for the first time that ceritinib is active on the R1275Q activation mutant (34). Only the G1202R resistance mutation is not well-targeted by any of the four inhibitors (Fig. 3B).

Two cell lines in the Oncolines panel have the NPM-ALK translocation: the lymphoma lines SR and SU-DHL-1. Consistently, these are the two most potently inhibited in the cell panel (Fig. 3C). The cellular potency order does not correspond to biochemical activity as the antiproliferative IC_{50}s on the SR and SU-DHL-1 cell lines are better for brigatinib and crizotinib compared with the other drugs (Supplementary Table S3). Based on IC_{50} ratios (calculated from log-averages), brigatinib (52-fold) and alectinib (20-fold) most selectively inhibit ALK-transformed cell lines, followed by ceritinib (15-fold) and crizotinib (11-fold). This order of relative potencies is in agreement with earlier work using the artificial BaF3 expression system (35).

The high cellular selectivity of brigatinib shows that spectrum-selective compounds can have very targeted effects in cellular systems, provided that they are potent. In this, brigatinib resembles the ABL inhibitor dasatinib (14). The cellular selectivity of

Downloaded from http://aacrjournals.org/mct/article-pdf/18/2/470/1860496/470.pdf by guest on 08 August 2023

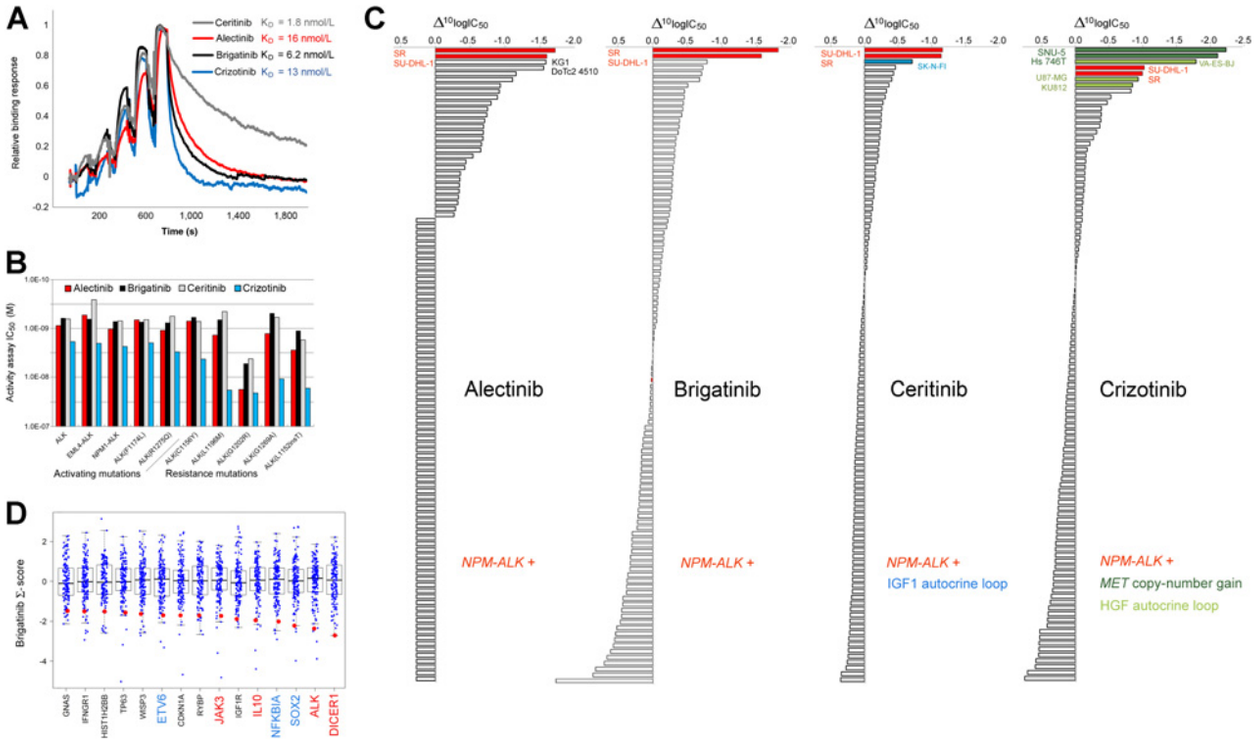

Figure 3.

Analysis of ALK inhibitors. **A,** SPR-binding assay on immobilized ALK cytoplasmic domain (residues 1058–1620). Kinetic parameters are given in Supplementary Table S5. **B,** Biochemical IC_{50}s of ALK inhibitors in various clinically occurring ALK variants. **C,** Waterfall plots of potencies in the cell panel. Geometrically averaged IC_{50}s are 17, 1.3, 2.7, and 1.9 μmol/L for alectinib, brigatinib, ceritinib, and crizotinib, respectively. Brigatinib is the most selective inhibitor of cell lines with the NPM-ALK translocation (red). Crizotinib also targets cell lines with *MET* copy-number gain (green). **D,** Correlation analysis of drug sensitivity and basal gene expression levels in the cell lines, as outlined in Fig. 2E, for the cellularly most selective ALK inhibitor brigatinib. The 15 most negative scores are shown, indicating correlation between high mRNA expression levels and low (potent) ^{10}logIC$_{50}$. Genes highlighted blue are validated as described in Fig. 2E. Genes highlighted red are also validated for alectinib or ceritinib.

alectinib provides evidence that biochemical selectivity can translate into a more specific targeting of oncogenic drivers. A recent meta-analysis of ALK inhibitor data indicated that alectinib actually also has the mildest toxicity profile in the clinic (36).

In some cases, cellular selectivity is confounded by off-target activities. Ceritinib, a known IGF1-R inhibitor (37), also inhibits SK-N-FI, which uses an IGF1 autocrine loop for growth (38). Consistently, high *IGF1R* mRNA expression correlates with ceritinib sensitivity (Supplementary Table S4). Crizotinib, originally developed as an MET inhibitor, inhibits cMET-amplified cell lines and those with an HGF autocrine loop (HGF is a ligand of cMET; Fig. 3C). However, not all cellular activities can be explained in this way, especially the sensitivities of the KG1 and DoTc2 4510 lines for alectinib (Fig. 3C).

To further investigate the mechanistic basis of these potency differences, we searched for additional drug response markers. Although the mutation analysis yielded no significant results (Supplementary Fig. S3D–S3G), we were able to validate expression of *ALK*, *IL10*, *DICER1*, and *JAK3*, as response markers (Fig. 3D). High *ALK* expression is a direct result of the NPM-ALK translocation. Across the 1000-cell line CCLE dataset (9), *IL10* and *DICER1* mRNA expressions are significantly correlated with *ALK* expression ($P < 4{\cdot}10^{-7}$), suggesting they cooperate with *ALK* as oncogenic drivers. *JAK3* is known to play an accessory role in ALK-driven lymphoma (39). Brigatinib and crizotinib have additional activity on JAK3, in contrast to ceritinib and alectinib which might explain their relatively potent cellular activity on NPM-ALK–driven lines.

The BTK inhibitors acalabrutinib and ibrutinib

BTK plays a crucial role in B-cell receptor activation and has been recognized as an oncogenic driver of several B-cell malignancies (40). At the moment, ibrutinib has been FDA-approved for mantle cell lymphoma and several leukemias. Acalabrutinib has been approved for mantle cell lymphoma. Trials are ongoing in other types of B-cell malignancies, such as follicular lymphoma (41).

Both inhibitors bind covalently to a cysteine in the active site of BTK, which is reflected by potent IC_{50}s in a kinase enzyme assay, even with a short incubation time, and confirmed in SPR-binding experiments (Fig. 4A). Our data confirm that acalabrutinib is more selective than ibrutinib (42). Ibrutinib inhibits 16 kinases by more than 95% at 1 μmol/L (Fig. 1A; Supplementary Table S2). Most of these are kinases with a cysteine in the active site, such as EGFR, HER2, and HER4 (the protein products of the *EGFR*, *ERBB2*, and *ERBB4* genes), but not all, such as VEGFR2, PDGFRα, and FGFR. In contrast, acalabrutinib only inhibits 2 kinases in the panel by more than 95% at 1 μmol/L, i.e., BTK and TEC. This is

Downloaded from http://aacrjournals.org/mct/article-pdf/18/2/470/1860496/470.pdf by guest on 08 August 2023

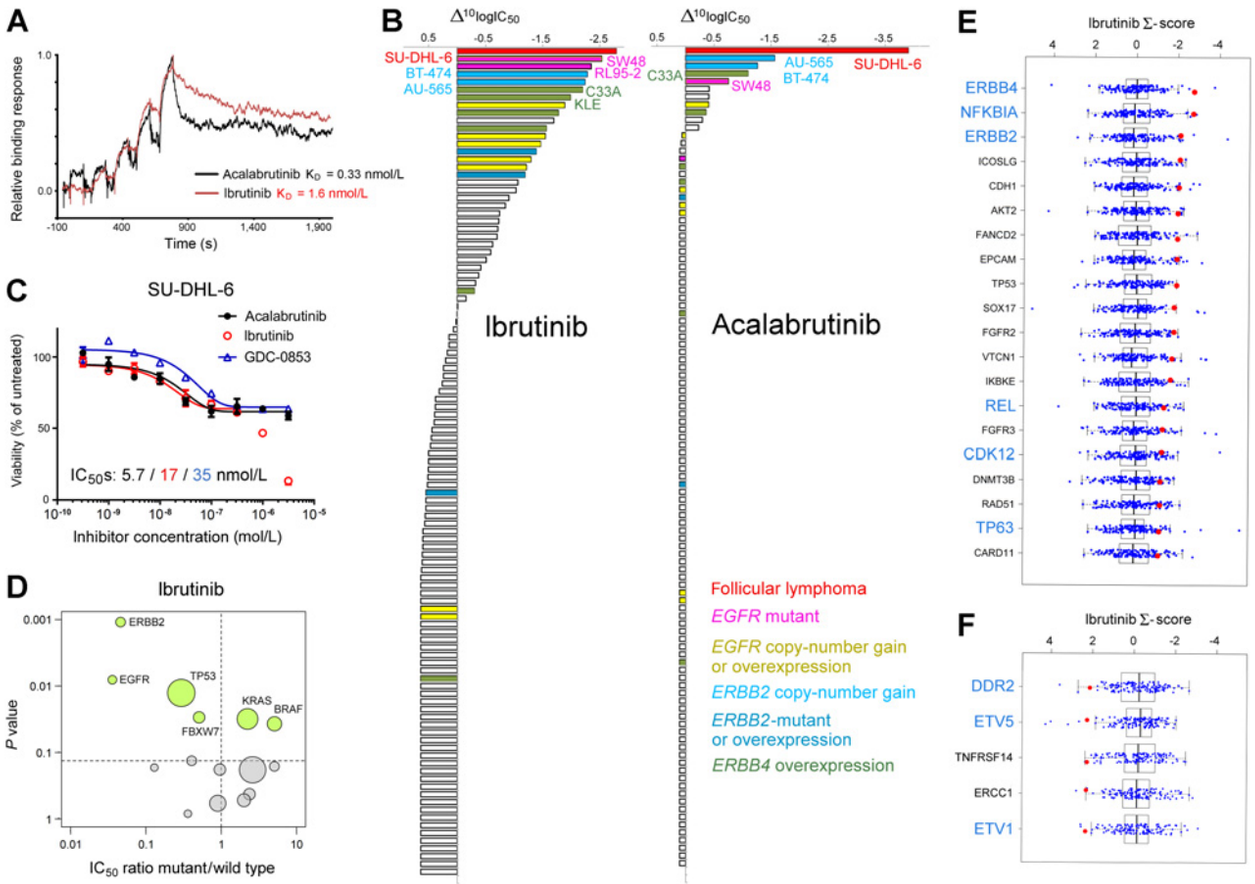

Figure 4.

Analysis of BTK inhibitors. **A,** SPR profiles binding to immobilized full-length BTK. **B,** Waterfall plots of potencies in the cell panel. Relevant tissue types or genetic changes are indicated by colors for each cell line. Overexpression refers to mRNA levels and is defined as a z-score $\geq$ 1.96 (equivalent to $P \leq 0.05$) in the CCLE or, if not available there, if gene overexpression is indicated in the COSMIC database (z-score > 2). Geometrically averaged IC$_{50}$s in the panel are 7.3 μmol/L for ibrutinib and 25 μmol/L for acalabrutinib. **C,** Proliferation assays of SU-DHL-6 demonstrating reproducible, partial inhibition (GDC-0853 is a selective BTK inhibitor in discovery phase). **D,** ANOVA analysis relating ibrutinib response to hotspot cancer gene mutations and copy-number variations in cell lines. See Fig. 2C for details. **E,** Highest correlations of drug sensitivity and basal gene expression levels, as outlined in Fig. 2E. **F,** As in **E**, but displaying the five most negative correlations. Genes highlighted blue are also significant using other gene expression databases and the ibrutinib data in PharmacoDB. For acalabrutinib, no response marker analysis is shown because it only inhibits one cell line.

reflected in the substantial selectivity entropy differences between acalabrutinib (S_{sel} = 1.4) and ibrutinib (S_{sel} = 2.4; Table 1).

The higher biochemical kinase selectivity of acalabrutinib is reflected in its cell panel profile. Acalabrutinib only inhibits SU-DHL-6, a follicular lymphoma cell line, with an IC$_{50}$ of < 100 nmol/L, whereas ibrutinib inhibits the proliferation of eight cell lines, among which SU-DHL-6 (Fig. 4B).

The effect on SU-DHL-6 is unexpected, because it is classified as a germinal center B-cell subtype of diffuse large B-cell lymphomas, which are considered unresponsive to BTK inhibitors (40). We verified inhibition of SU-DHL-6 (a partial effect of ~40%) with the BTK inhibitor GDC-0853, which is chemically unrelated to the other two (Fig. 4C). SU-DHL-6 bears some hallmarks of the BTK inhibitor–responsive ABC-subtype, notable expression of *IRF4*, *SPIB*, and *PIM* (9). A more precise definition of the BTK inhibitor responder genotype seems needed.

Because acalabrutinib only inhibits one single-cell line in the panel, drug sensitivity analysis is less informative. For ibrutinib, analysis of hotspot mutations and copy-number variations reveals, a.o., amplification of *ERBB2* (Fig. 4D), which is one of the off-targets of ibrutinib (Supplementary Table S2; ref. 43). Also from gene expression analysis, *ERBB2* is one of the most significant sensitivity markers (Fig. 4E). Thus, the cell panel profiling experiments support clinical trials of ibrutinib in HER2-driven cancers, such as *ERBB2*-amplified esophagogastric carcinoma (NCT02884453).

The most significant gene expression–based marker for ibrutinib is *ERBB4*, also an off-target (Fig. 4E). This supports the application of ibrutinib in *ERBB4*-overexpressing cancers (44). Other validated potential response and resistance biomarkers are indicated in Fig. 4E and F.

The EGFR inhibitor osimertinib

Osimertinib is a covalent EGFR inhibitor that was approved by the FDA in 2017 for treatment of EGFR(T790M)-mutant lung cancer. It was designed to potently and selectively inhibit EGFR

Downloaded from http://aacrjournals.org/mct/article-pdf/18/2/470/1860496/470.pdf by guest on 08 August 2023

(T790M), a frequently occurring resistance mutation after treatment with first-line EGFR inhibitors (45).

It has been claimed that osimertinib is selective for EGFR (T790M) (45). However, in the kinase assays, it has similar activities on wild-type and T790M-mutant EGFR, in presence and absence of activating mutations (Table 1; Fig. 5A). First-generation inhibitors such as erlotinib and gefitinib are respectively 600 or 2,500 times less potent on the T790M variants (Fig. 5A). In general, osimertinib is less selective than first-generation inhibitors, inhibiting 11 kinases with >95% at 1 μmol/L (ACK, ALK, BRK, HER2, HER4, JAK3, LTK, MNK1/2, TNK1, and ROS; Supplementary Table S2). This supports earlier work (15, 45) and is also apparent from osimertinib's selectivity entropy of 2.1, compared with 1.0, 0.5, and 0.5, for afatinib, erlotinib, and gefitinib, respectively (Table 1; ref. 14).

Consistent with the clinical indication, osimertinib targets the two cell lines with EGFR driver mutations in the panel (SW48 and RL95-2) with approximately 33 times more potent IC_{50} than non–EGFR-mutant lines (Fig. 5B). The most osimertinib-sensitive line is RL95-2, which contains the EGFR(A289V) ectodomain mutation. The cell line SW48, which contains the EGFR(G719S)-activating mutation, is 2-fold less sensitive. In contrast, RL95-2 is 8-fold less sensitive than SW48 to erlotinib and gefitinib (Supplementary Fig. S4A and S4B), indicating that osimertinib might be particularly effective in targeting ectodomain mutations.

In line with osimertinib's biochemical inhibition of HER2, also cell lines with *ERBB2* amplification and high *ERBB2* gene expression levels are sensitive (Figs. 1 and 5B). Because osimertinib was designed to avoid the kinase gatekeeper region, it might be useful against *ERBB2*-driven cancers with gatekeeper mutations such as HER2(T798I), which was recently observed in neratinib-treated patients (46).

The HER2 inhibitor neratinib

Neratinib was approved in 2017 for HER2-positive breast cancer. It is a covalently binding drug that inhibits HER2 and, even more potently, EGFR (Table 1; Fig. 1). In addition, neratinib inhibits HER4, MST3, MST4, and LOK by more than 95% at 1 μmol/L (Supplementary Table S2). Its selectivity entropy of 1.6 indicates moderate selectivity (Table 1).

In the cell line panel, neratinib targets *ERBB2*-amplified breast cancer cell lines such as AU-565 and BT-474 (Fig. 5B), which on average are 95-fold more sensitive than the other cell lines (ratio of log-averaged IC_{50}s). Because *ERBB2*-amplified cell lines highly express *ERBB2*, this is also the most significant gene expression–based marker (Fig. 5F). Also *EGFR* gene expression predicts drug sensitivity to neratinib (Fig. 5F).

Neratinib's drug action is best compared with that of lapatinib, a noncovalent HER2 inhibitor that is also approved for HER2-positive breast cancer. Although lapatinib is biochemically more potent and selective ($IC_{50,ERBB2}$ = 9.8 nmol/L, S_{sel} 1.0; ref. 14), it targets *ERBB2*-amplified lines with a 27-fold IC_{50} ratio (Supplementary Table S3). The increased cellular selectivity of neratinib supports the ongoing head-to-head clinical trial with lapatinib (NCT01808573; ref. 47).

Novel drug response biomarkers for EGFR/HER2 inhibitors

Not all responses of cell lines to osimertinib or neratinib can be explained by *EGFR* or *ERBB2* activation (45, 47). Mutation hotspot analysis shows *SMAD4* loss and *FBXW7* mutation as additional genomic response markers for both inhibitors, and *KRAS* mutation as resistance marker (Fig. 5C and D). To deconvolute whether these are EGFR or HER2 related, we profiled additional FDA-approved therapy including the highly selective EGFR inhibitor erlotinib and the anti-HER2 antibody herceptin in 102 cell lines (Supplementary Fig. S4A). Apparently, *FBXW7* mutation sensitizes to EGFR inhibition, whereas *KRAS* mutation is an HER2 inhibitor–related marker, in agreement with earlier work (14). *SMAD4* is also a marker for afatinib response. Across 1,000 cell lines (9), low *FBXW7* expression correlates significantly with high *EGFR* expression ($P < 2{\cdot}10^{-25}$), and low *SMAD4* with high *ERBB2* ($P < 2{\cdot}10^{-23}$) and *EGFR* expression ($P < 2{\cdot}10^{-46}$) which substantiates a mechanistic connection.

Our gene expression–based marker workflow suggests *FGFR2*, *FGFR3*, *NFKBIA*, and *TP63* as additional sensitivity markers for osimertinib, even though the drug does not inhibit FGFRs (Fig. 5E). These genes were validated in 102 cell line profiles of erlotinib and gefitinib, and in independent pharmacogenomic datasets of these drugs (Supplementary Table S4), making them interesting for follow-up studies. FOXA1 was independently validated as a sensitivity marker for neratinib (Fig. 5F).

The MEK inhibitor cobimetinib

In 2015, the FDA approved cobimetinib for the treatment of BRAF(V600E)- and BRAF(V600K)-mutant melanoma in combination with the BRAF inhibitor vemurafenib (Zelboraf), which followed the earlier approval of the MEK inhibitor trametinib (Mekinist) in combination with the BRAF inhibitor dabrafenib (Tafinlar).

Cobimetinib is very selective for MEK1 and MEK2 (Table 1), with only additional activity on MEKK1, leading to a very low selectivity entropy of 0.8 (Table 1). This is due to its unique type III allosteric binding mode, which it shares with trametinib (48). Cobimetinib is less potent but somewhat more selective compared with trametinib ($IC_{50,MEK1}$ = 17 nmol/L, $IC_{50,MEK2}$ = 42 nmol/L, S_{sel} = 1.3; ref. 14). Both drugs partially inhibit BRAF and RAF1 at 1 μmol/L (Supplementary Table S2), which could contribute to their efficacy.

Consistent with its clinical label, the cellular profile of cobimetinib shows high activity on BRAF(V600E)-mutant cell lines, and the BRAF(V487-P492>A)-mutant BxPC-3 line (Fig. 5G and H). These show on average a 21-fold better sensitivity than wild-type lines (^{10}log-averaged IC_{50}s). This is in the same range as trametinib (16-fold IC_{50} difference; Supplementary Fig. S5A). For comparison, the BRAF inhibitor dabrafenib shows a 56-fold IC_{50} difference between BRAF(V600E) and BRAF wild-type lines in a 102-cell line profiling (Supplementary Fig. S5A).

Another well-known MEK response marker that has been evaluated in clinical trials is *RAS* mutation (48). Cobimetinib also targets *RAS*-mutant cell lines in the Oncolines panel (Fig. 5G), although the average sensitivity difference is only 2.3-fold between KRAS-mutant and wild-type cell lines. This is similar for trametinib (Supplementary Fig. S5B). This relatively poor cellular selectivity window might in part explain why clinical trials of MEK inhibitors in *RAS*-mutant patients have failed (48).

Based on basal gene expression, *ETV4* and *ETV5* can be validated as sensitivity markers, and *BARD1*, *AKT2*, and *BCL6* as resistance markers (Fig. 5I). These are consistent with both internal and independent pharmacogenomic profiling of trametinib (Supplementary Table S4). *ETV4* and *ETV5* are transcriptional targets of MEK/ERK signaling and were previously identified as sensitivity markers for selumetinib, another MEK inhibitor (49).

Downloaded from http://aacrjournals.org/mct/article-pdf/18/2/470/1860496/470.pdf by guest on 08 August 2023

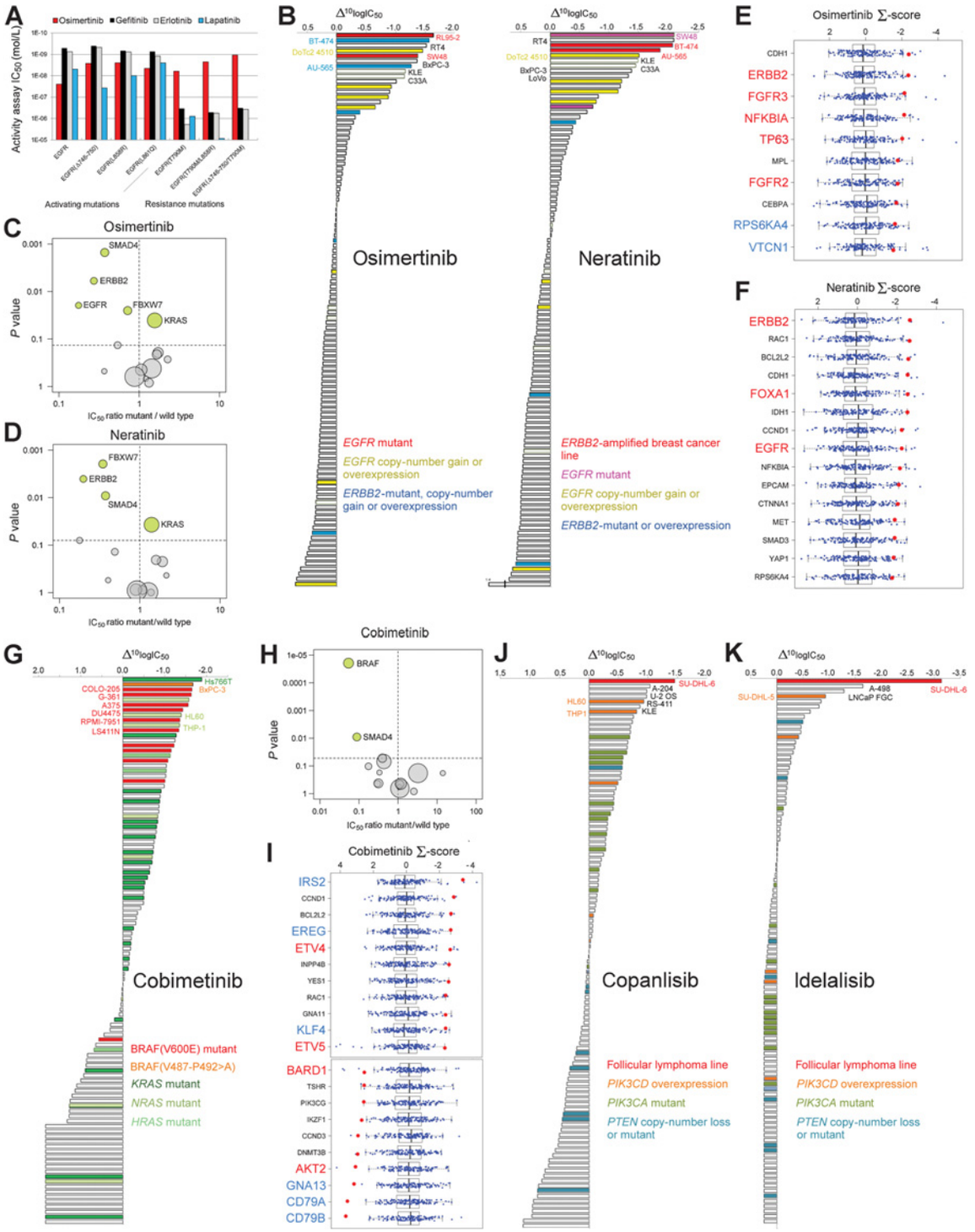

Figure 5.

Analysis of EGFR, HER2, MEK, and PI3K inhibitors. **A,** Biochemical IC_{50}s of osimertinib on various clinically occurring activating and resistance variants of EGFR. Data for gefitinib, erlotinib, and lapatinib in the same panel are taken from ref. 19. **B,** Waterfall plots of EGFR/HER2 inhibitors in the cell panel. Coloring as in Fig. 4B. Geometrically averaged IC_{50}s in the panel ($IC_{50,average}$) are 2.1 μmol/L for osimertinib and 1.2 μmol/L for neratinib. **C** and **D,** ANOVA analysis relating osimertinib and neratinib responses to hotspot cancer gene mutations and copy-number variations in cell lines. See Fig. 2C for details. **E,** Correlation analysis of osimertinib sensitivity and basal gene expression levels in the cell lines. See Fig. 2E for details. Genes highlighted in blue are also significant using other gene expression databases and, if present, in the PharmacoDB. Genes highlighted red can also be validated in a similar way for erlotinib or gefitinib. **F,** As in **E** but for neratinib. Genes highlighted red are also validated for lapatinib. **G,** Waterfall plot of cobimetinib in the cell panel. $IC_{50,average}$ is 457 nmol/L. **H,** ANOVA analysis for cobimetinib response. **I,** As in **E** but for cobimetinib. Genes highlighted red are also validated for trametinib. *BCL6* is not shown here. **J** and **K,** Waterfall plots of PI3K inhibitors in the cell panel. $IC_{50,average}$s are 114 nmol/L for copanlisib and 18.1 μmol/L for idelalisib.

Downloaded from http://aacrjournals.org/mct/article-pdf/18/2/470/1860496/470.pdf by guest on 08 August 2023

The PI3K inhibitors copanlisib and idelalisib

The profiling also includes the first two clinically approved inhibitors of PI3Ks: copanlisib, a PI3Kα inhibitor, and idelalisib, a PI3Kδ inhibitor. Both are used to treat follicular lymphoma, with idelalisib also having additional indications. PI3kinases are lipid kinases, not protein kinases, and consistently both inhibitors have no activity in the biochemical assay panel (Fig. 1A). To study their target affinity, we profiled both inhibitors with SPR. Immobilized PI3Ks consisted of p110α, -β, -γ, or -δ catalytic subunits bound to the p85α regulatory subunit (Table 1; Supplementary Table S5). This shows that copanlisib is a pan-PI3K inhibitor and idelalisib a selective PI3Kδ inhibitor.

Both drugs are most active on the SU-DHL-6 cell line, which is the only line of follicular lymphoma origin (Fig. 5J and K). Copanlisib and idelalisib have, respectively, a 29- and 1,440-fold more potent IC_{50} on SU-DHL-6 than nonfollicular lines. For idelalisib, this selective cellular response reflects its biochemical selectivity. SU-DHL-6 contains a p110δ(E83K) mutation (8), which is involved in activated PI3 kinase δ syndrome. For copanlisib, *PIK3CA*-mutant cells are 2.2-fold more sensitive than nonmutant lines, which is significant in a *t* test ($P < 0.05$; Fig. 5J). *PIK3CA* targeting was also seen for the PI3Kα inhibitor alpelisib (13). Other markers are given in Supplementary Table S4.

Multikinase inhibitors

Finally, we profiled four newly approved inhibitors which are spectrum selective: the angiogenesis inhibitors lenvatinib, nintedanib, tivozanib, and the FLT3 inhibitor midostaurin. Biochemically, lenvatinib is the most selective of the angiogenesis inhibitors ($S_{sel} = 2.0$), whereas midostaurin is the least selective of the entire kinase inhibitor set ($S_{sel} = 3.4$; Table 1). As a result of spectrum-selectivity, cellular inhibition profiles are determined by off-target effects. For profiles and analysis, see Supplementary Tables S2 and S3 and Supplementary Fig. S6A and S6B. Notably, midostaurin is very active on cell lines that overexpress *PDGFRB*, which it also potently inhibits biochemically (Supplementary Table S4).

Biomarker sensitivity and specificity

As last step, we reanalyzed all validated biomarkers in a binary way. We divided cell lines into responders and nonresponders and calculated the sensitivity and specificity of response predictors (Supplementary Table S6). Almost all clinically-used markers score high, even though we only use *in vitro* data. Other markers might need combination to meet selectivity and specificity thresholds, for instance those for CDK4/6 inhibitors.

Conclusion

We present the combined profiling of approved kinase inhibitors on a biochemical assay panel of 280 kinases and in a proliferation assay panel of 108 cancer cell lines. The comprehensive selectivity data will contribute to repurposing approved drugs for cancer or other diseases. For instance, CLK1 is an important target for Duchenne muscular dystrophy (50), which is strongly inhibited by ceritinib, brigatinib, abemaciclib, and palbociclib. High expression of *ERBB4*, encoding HER4, is a recently discovered oncogenic driver (44) and is inhibited by ibrutinib, neratinib, brigatinib, and osimertinib.

The data will also help to further define patient populations that can benefit from kinase inhibitor treatment. For most drugs, the tissues and mutations described in the FDA labels correspond to the molecular characteristics of the most sensitive cell lines, demonstrating the translational utility of cell panel profiling. For markers used for therapeutic decisions, such as BRAF(V600E), ALK translocation, or *ERBB2* amplification, inhibitors show between 11-fold (crizotinib) and 95-fold (neratinib) potency difference between biomarker-positive and -negative cells. For markers that failed to meet endpoints in clinical trials, this potency window is lower, e.g., 2.3-fold for *KRAS* mutation and cobimetinib and 2.7-fold for *CDKN2A* loss for CDK4/6 inhibitors. This suggests that a high sensitivity window in cell panel profiling is a prerequisite for clinical success of targeted therapy. Combination of markers, such as *CDKN2A*, *RB1*, and *TP53* status for CDK4/6 inhibitors, would be a viable strategy to prove efficacy in new patient populations.

Disclosure of Potential Conflicts of Interest

No potential conflicts of interest were disclosed.

Authors' Contributions

Conception and design: J.C.M. Uitdehaag, J.J. Kooijman, G.J.R. Zaman
Development of methodology: J.C.M. Uitdehaag, J.J. Kooijman
Acquisition of data (provided animals, acquired and managed patients, provided facilities, etc.): J.C.M. Uitdehaag, J.J. Kooijman, J.A.D.M. de Roos, M.B.W. Prinsen, J. Dylus, N. Willemsen-Seegers, M. Sawa, J. de Man, R.C. Buijsman, G.J.R. Zaman
Analysis and interpretation of data (e.g., statistical analysis, biostatistics, computational analysis): J.C.M. Uitdehaag, J.J. Kooijman, J.A.D.M. de Roos, M.B.W. Prinsen, J. Dylus, N. Willemsen-Seegers, S.J.C. van Gerwen, G.J.R. Zaman
Writing, review, and/or revision of the manuscript: J.C.M. Uitdehaag, J.J. Kooijman, G.J.R. Zaman
Administrative, technical, or material support (i.e., reporting or organizing data, constructing databases): J.C.M. Uitdehaag, J.J. Kooijman, Y. Kawase
Study supervision: G.J.R. Zaman

Acknowledgments

We thank Judith de Vetter for contributing to the cellular profiling and Biacore experiments.

The costs of publication of this article were defrayed in part by the payment of page charges. This article must therefore be hereby marked *advertisement* in accordance with 18 U.S.C. Section 1734 solely to indicate this fact.

Received August 3, 2018; revised September 17, 2018; accepted October 23, 2018; published first October 31, 2018.

References

1. Weinstein IB. Disorders in cell circuitry during multistage carcinogenesis: the role of homeostasis. Carcinogenesis 2000;21:857–64.
2. Lynch TJ, Bell DW, Sordella R, Gurubhagavatula S, Okimoto RA, Brannigan BW, et al. Activating mutations in the epidermal growth factor receptor underlying responsiveness of non-small-cell lung cancer to gefitinib. N Engl J Med 2014;350:2129–39.
3. Yang H, Higgins B, Kolinsky K, Packman K, Go Z, Iyer R, et al. RG7204 (PLX4032), a selective BRAFV600E inhibitor, displays potent antitumor activity in preclinical melanoma models. Cancer Res 2010;70:5518–27.
4. Kwak EL, Bang YJ, Camidge DR, Shaw AT, Solomon B, Maki RG, et al. Anaplastic lymphoma kinase inhibition in non-small-cell lung cancer. N Engl J Med 2010;363:1693–703.

Downloaded from http://aacrjournals.org/mct/article-pdf/18/2/470/1860496/470.pdf by guest on 08 August 2023

5. Sosman JA, Kim KB, Schuchter L, Gonzalez R, Pavlick AC, Weber JS, et al. Survival in BRAF V600-mutant advanced melanoma treated with vemurafenib. N Engl J Med 2012;366:707–14.
6. Krop IE, Mayer IA, Ganju V, Dickler M, Johnston S, Morales S, et al. Pictilisib for oestrogen receptor-positive, aromatase inhibitor-resistant, advanced or metastatic breast cancer (FERGI): a randomized, double-blind, placebo-controlled, phase 2 trial. Lancet Oncol 2016;17:811–21.
7. Barretina J, Caponigro G, Stransky N, Venkatesan K, Margolin AA, Kim S, et al. The cancer cell line encyclopedia enables predictive modelling of anticancer drug sensitivity. Nature 2012;483:603–7.
8. Iorio F, Knijnenburg TA, Vis DJ, Bignell GR, Menden MP, Schubert M, et al. A landscape of pharmacogenomic interactions in cancer. Cell 2016;166:740–54.
9. Rees MG, Seashore-Ludlow B, Cheah JH, Adams DJ, Price EV, Gill S, et al. Correlating chemical sensitivity and basal gene expression reveals mechanism of action. Nature Chem Biol 2015;12:109–16.
10. Eisen T, Ahmad T, Flaherty KT, Gore M, Kaye S, Marais R, et al. Sorafenib in advanced melanoma: a phase II randomised discontinuation trial analysis. Br J Cancer 2006;95:581–6.
11. Antolin AA, Workman P, Mestres J, Al-Lazikani B. Polypharmacology in precision oncology: current applications and future prospects. Curr Pharm Design 2016;22:6935–45.
12. Davis MI, Hunt JP, Herrgard S, Ciceri P, Wodicka LM, Pallares G, et al. Comprehensive analysis of kinase inhibitor selectivity. Nat Biotech 2011;29:1046–51.
13. Uitdehaag JC, de Roos JA, Prinsen MB, Willemsen-Seegers N, de Vetter JR, Dylus J, et al. Cell panel profiling reveals conserved therapeutic clusters and differentiates the mechanism of action of different PI3K/mTOR, Aurora kinase and EZH2 inhibitors. Mol Cancer Ther 2016;15:3097–109.
14. Uitdehaag JC, de Roos JA, van Doornmalen AM, Prinsen MB, de Man J, Tanizawa Y, et al. Comparison of the cancer gene targeting and biochemical selectivities of all targeted kinase inhibitors approved for clinical use. PLoS One 2014;9:e92146.
15. Klaeger S, Heinzlmeier S, Wilhelm M, Polzer H, Vick B, Koenig PA, et al. The target landscape of clinical kinase drugs. Science 2017;358:6367–83.
16. Chang MT, Asthana S, Gao SP, Lee BH, Chapman JS, Kandoth C, et al. Identifying recurrent mutations in cancer reveals widespread lineage diversity and mutational specificity. Nat Biotech 2016;34:155–63.
17. Klijn C, Durinck S, Stawiski EW, Haverty PM, Jiang Z, Liu H, et al. A comprehensive transcriptional portrait of human cancer cell lines. Nat Biotech 2015;33:306–12.
18. Smirnov P, Kofia V, Maru A, Freeman M, Ho C, et al. PharmacoDB: an integrative database for mining in vitro anticancer drug screening studies. Nucleic Acids Res 2018;46:D994–D1002.
19. Kitagawa D, Yokota K, Gouda M, Narumi Y, Ohmoto H, Nishiwaki E, et al. Activity-based kinase profiling of approved tyrosine kinase inhibitors. Genes Cells 2013;18:110–22.
20. Willemsen-Seegers N, Uitdehaag JC, Prinsen MB, de Vetter JR, de Man J, Sawa M, et al. Compound selectivity and target residence time of kinase inhibitors studied with surface plasmon resonance. J Mol Biol 2016;429:574–86.
21. Lee JC, Vivanco I, Beroukhim R, Huang JH, Feng WL, DeBiasi RM, et al. Epidermal growth factor receptor activation in glioblastoma through novel missense mutations in the extracellular domain. PLoS Med 2006;3:e485.
22. Cotto KC, Wagner AH, Feng YY, Kiwala S, Coffman AC, Spies G, et al. DGIdb 3.0: a redesign and expansion of the drug-gene interaction database. Nucleic Acids Res 2018;46:D1069–73.
23. Tripathy D, Bardia A, Sellers WR. Ribociclib (LEE011): mechanism of action and clinical impact of this selective cyclin-dependent kinase 4/6 inhibitor in various solid tumors. Clin Cancer Res 2017;23:3251–62.
24. Chen P, Lee NV, Hu W, Xu M, Ferre RA, Lam H, et al. Spectrum and degree of CDK drug interactions predicts clinical performance. Mol Cancer Ther 2016;15:2273–81.
25. Xu H, Yu S, Liu Q, Yuan X, Mani S, Pestell RG, et al. Recent advances of highly selective CDK4/6 inhibitors in breast cancer. J Hematol Oncol 2017;10:97–109.
26. Reya T, Duncan AW, Ailles L, Domen J, Scherer DC, Willert K, et al. A role for Wnt signalling in self-renewal of haematopoietic stem cells. Nature 2003;423:409–14.
27. Cousins EM, Goldfarb D, Yan F, Roques J, Darr D, Johnson GL, et al. Competitive kinase enrichment proteomics reveals that abemaciclib inhibits GSK3β and activates Wnt signalling. Mol Cancer Res 2017;16:333–44.
28. Garrido-Castro AC, Goel S. CDK4/6 inhibition in breast cancer: mechanism of response and treatment failure. Curr Breast Cancer Rep 2017;9:26–33.
29. Rader J, Russell MR, Hart LS, Nakazawa MS, Belcastro LT, Martinez D, et al. Dual CDK4/CDK6 inhibition induces cell cycle arrest and senescence in neuroblastoma. Clin Cancer Res 2013;19:6173–82.
30. Vijayaraghavan S, Karakas C, Doostan I, Chen X, Bui T, Yi M, et al. CDK4/6 and autophagy inhibitors synergistically induce senescence in Rb positive cytoplasmic cyclin E negative cancers. Nat Commun 2017;8:15916.
31. Patnaik A, Rosen LS, Tolaney SM, Tolcher AW, Goldman JW, Gandhi L, et al. Efficacy and safety of abemaciclib, an inhibitor of CDK4 and CDK6, for patients with breast cancer, non-small cell lung cancer, and other solid tumors. Cancer Discov 2016;6:740–53.
32. Herrera-Abreu MT, Palafox M, Ashgar U, Rivas MA, Cutts RJ, Garcia-Murillas I, et al. Early adaptation and acquired resistance to CDK4/6 in estrogen receptor-positive breast cancer. Cancer Res 2016;76:2301–13.
33. Mossé YP, Voss SD, Lim MS, Rolland D, Minard CG, Fox E, et al. Targeting ALK with crizotinib in pediatric anaplastic large cell lymphoma and inflammatory myofibroblastic tumor: a children's oncology study group. J Clin Oncol 2017;35:3215–21.
34. Friboulet L, Li N, Katayama R, Lee CC, Gainor JF, Crystal AS, et al. The ALK inhibitor ceritinib overcomes crizotinib resistance in non-small cell lung cancer. Cancer Discov 2014;4:662–73.
35. Zhang S, Anjum R, Squillace R, Nadworny S, Zhou T, Keats J, et al. The potent ALK inhibitor brigatinib (AP26113) overcomes mechanisms of resistance to first- and second-generation ALK inhibitors in preclinical models. Clin Cancer Res 2016;22:5527–38.
36. Hong S, Zhang L. Evaluation of toxicity profile of ALK inhibitors in non-small cell lung cancer (NSCLC), J. Thoracic Oncol 2017;12:S2392, abstract PUB081.
37. Wilson C, Nimick M, Nehoff H, Ashton JC. ALK and IGF-1R as independent targets in crizotinib resistant lung cancer. Sci Rep 2017;7;13955.
38. Pappano WN, Jung PM, Meulbroek JA, Wang YC, Hubbard RD, Zhang Q, et al. Reversal of oncogene transformation and suppression of tumor growth by the novel IGF1R kinase inhibitor A-928605. BMC Cancer 2009;9:314.
39. Lai R, Rassidakis GZ, Lin Q, Atwell C, Medeiros J, Amin HM. Jak3 activation is significantly associated with ALK expression in anaplastic large cell lymphoma. Hum Pathol 2005;36:939–44.
40. Davis RE, Ngo VN, Lenz G, Tolar P, Young RM, Romessere PB, et al. Chronic active B-cell-receptor signalling in diffuse large B-cell lymphoma. Nature 2010;463;88–92.
41. Bartlett NL, Costello BA, LaPlant BR, Ansell SM, Kuruvilla JG, Reeder CB, et al. Single agent ibrutinib in relapsed or refractory follicular lymphoma: a phase 2 consortium trial. Blood 2018;131:182–90.
42. Byrd JC, Harrington B, O'Brien S, Jones JA, Schuh A, Devereux S, et al. Acalabrutinib (ACP-196) in relapsed chronic lymphocytic leukemia. N Engl J Med 2016;374:323–32.
43. Grabinski N, Ewald F. Ibrutinib (Imbruvica™) potently inhibits ErbB receptor phosphorylation and cell viability of ErbB2-positive breast cancer cells. Invest New Drugs 2014;32:1096–104.
44. Rauf F, Festa F, Park JG, Magee M, Eaton S, Rinaldi C, et al. Ibrutinib inhibition of ERBB4 reduces cell growth in a WNT5A-dependent manner. Oncogene 2018;37:2237–50.
45. Cross DA, Ashton SE, Ghiorghiu S, Eberlein C, Nebhan CA, Spitzler PJ, et al. AZD9291 an irreversible EGFR TKI overcomes T790M-mediated resistance to EGFR inhibitors in lung cancer. Cancer Discov 2014;4:1046–61.
46. Hanker AB, Brewer MR, Sheehan JH, Koch JP, Sliwoski GR, Nagy R, et al. An acquired HER2(T798I) gatekeeper mutation induces resistance to

Downloaded from http://aacrjournals.org/mct/article-pdf/18/2/470/1860496/470.pdf by guest on 08 August 2023

neratinib in a patient with HER2 mutant-driven breast cancer. Cancer Discov 2017;7:575–85.
47. Feldinger K, Kong A. Profile of neratinib and its potential in the treatment of breast cancer. Breast Cancer 2015;7:147–62.
48. Cheng Y, Tian H. Current development status of MEK inhibitors. Molecules 2017;22:1551.
49. Dry JR, Pavey S, Pratilas CA, Harbron C, Runswick S, Hodgson D, et al. Transcriptional pathway signatures predict MEK addiction and response to selumetinib (AZD6244). Cancer Res 2010;70:2264–73.
50. Sako Y, Ninomiya K, Okuno Y, Toyomoto M, Nishida A, Koike Y, et al. Development of an orally available inhibitor of CLK1 for skipping a mutated dystrophin exon in Duchenne muscular dystrophy. Sci Rep 2017;7:46126.

Downloaded from http://aacrjournals.org/mct/article-pdf/18/2/470/1860496/470.pdf by guest on 08 August 2023